Theory of hyperfine effects in the Zeeman splitting of the $2\,^3P$ state of Li^+ †

A. Norman Jette
Applied Physics Laboratory, The Johns Hopkins University, Silver Spring, Maryland 20910

Taesul Lee and T. P. Das
Department of Physics, State University of New York, Albany, New York 12222

(Received 15 October 1973)

The linked-cluster many-body perturbation theory is applied to the study of the one- and two-electron contributions to the magnetic contact, dipolar, and orbital hyperfine interaction in the $2\,^3P$ state of the $^6Li^+$ and $^7Li^+$ ions. The relative importance of one- and two-electron contributions to the various hyperfine constants are discussed, and comparisons are made between our theoretical results and recent experimental data obtained both by beam-foil spectroscopy and by radio-frequency resonance techniques utilizing electron-impact excitation.

I. INTRODUCTION

Because of the recent experimental work on the measurement of the hyperfine splittings in the $2\,^3P$ state of Li^+,[1,2] it has become desirable to have an accurate theory for the hyperfine coupling constants. The reasons for such a theory are twofold, one being the obvious comparison of theoretical and experimental splittings, while the other is to see if one can get accurate enough results in this two-electron system to draw conclusions about the role of relativistic and quantum electrodynamic corrections to the hyperfine constants. Such an analysis has already been done for the $2\,^3S$ state of ^3He, and it is interesting to extend it to the present isoelectronic system with a larger nuclear charge.[3]

To calculate the hyperfine splittings one can adopt one of two general approaches, the configuration-interaction method[4,5] or a perturbative scheme,[6-12] and with all of their ramifications these two procedures should be equivalent. An accurate theoretical analysis of the present system requires a detailed treatment of many-body (in the present case, two-body) effects. Because of past successes we made use of the linked-cluster many-body perturbation method (LCMBPT) for our calculation.[6-12] With this approach we obtained the individual contributions from the contact, dipolar, and orbital interactions to the energy levels, and as a byproduct of the calculation from a theoretical point of view, information on the convergence of the perturbation procedure and the relative importance of one- and two-electron contributions to the hyperfine constants.

Section II contains a brief description of the linked-cluster many-body method, a listing of individual diagrams, their physical meaning, their values, and the net contributions to the three hyperfine coupling constants from different orders of perturbation in nonrelativistic theory. The magnetic-field dependence of the energy levels is treated in Sec. III along with the comparison of the theoretical splittings with experiment. The contributions of the various corrections, both relativistic and nonrelativistic, alluded to above are discussed in Sec. IV with the results of the calculation.

II. ZERO FIELD-HYPERFINE INTERACTION

We will present a brief summary of the theoretical procedure to evaluate the hyperfine constants in the absence of an external magnetic field.[6-12] The total nonrelativistic Hamiltonian for an atomic system of N electrons is

$$\mathcal{H} = \sum_i T_i + \sum_{i>j} v_{ij}\,, \tag{1}$$

where T_i represents the sum of the kinetic energy and nuclear Coulomb potential of the ith electron and v_{ij} is the electrostatic interaction between electrons i and j. One is interested in the solution Ψ_0 of the Schrödinger equation

$$\mathcal{H}\Psi_0 = E\Psi_0\,. \tag{2}$$

In the perturbation procedure used here, one replaces the Hamiltonian $\mathcal{H}$ by a one-electron Hamiltonain $\mathcal{H}_0$:

$$\mathcal{H}_0 = \sum_i (T_i + V_i) \tag{3}$$

and treats $\mathcal{H}' = \mathcal{H} - \mathcal{H}_0$ as a perturbation. The single-particle potential V_i is selected in such a way that the one-electron equation

$$(T + V)\phi_i = \epsilon_i \phi_i \tag{4}$$

can be solved conveniently for a complete set of states with eigenvalues ϵ_i including the continuum. A normalized zero-order determinantal wave function Φ_0 can then be formed out of N of these one-electron states. Φ_0 satisfies the unperturbed Schrödinger equation

$$\mathcal{H}_0\Phi_0 = E_0\Phi_0 , \tag{5}$$

with $E_0 = \sum_i \epsilon_i$. Using the time-development-operator technique, one can find a perturbation expansion of Ψ_0, with Φ_0 as the zero-order approximation. Then the expectation value of an operator O:

$$\langle O\rangle = \langle\Psi_0|O|\Psi_0\rangle/\langle\Psi_0|\Psi_0\rangle$$

can be written as

$$\langle O\rangle = \sum_{n,m} \langle\Phi_0|[\mathcal{H}'(E_0-\mathcal{H}_0)^{-1}]^n \times O[(E_0-\mathcal{H}_0)^{-1}\mathcal{H}']^m|\Phi_0\rangle_L , \tag{6}$$

where L indicates that the summation is over linked terms only.

We can apply this procedure to the evaluation of the hyperfine constants in the excited $2\,^3P$ ($m_J = 2$) states of the Li^+ ion. With the usual V^{N-1} potential in Eq. (4), one gets the following radial equations for $P_{nl}(r)$ (r times radial wave function):

$$l=0:\ \left(\frac{d^2}{dr^2}+\frac{6}{r}-\frac{2}{r}\,Y_0(2p,2p;r)+2\epsilon_{ns}\right)P_{ns}(r) + \frac{2}{3r}\,Y_1(2p,ns;r)P_{2p}(r)=0 , \tag{7}$$

and for

$$l>0:\ \left(\frac{d^2}{dr^2}-\frac{l(l+1)}{r^2}+\frac{6}{r}-\frac{2}{r}\,Y_0(1s,1s;r)+2\epsilon_{nl}\right) \times P_{nl}(r)+\frac{2}{(2l+1)r}\,Y_l(1s,nl;r)P_{1s}(r)=0 , \tag{8}$$

where in the Hartree notation

$$Y_k(nl,n'l';r) = r\int_0^\infty \frac{r_<^k}{r_>^{k+1}} P_{nl}(r')P_{n'l'}(r')\,dr' .$$

Equations (7) and (8) are solved self-consistently for the $1s$ and $2p$ electrons. Higher excited orbitals are obtained with these $1s$ and $2p$ wave functions and the Y_k functions. We have included in our perturbation calculation one-particle excited states up to $l=3$. For each l we have generated bound states up to $n=10$ and continuum states at 12 different points in k space in such a way that we can use the Gauss-Laguerre quadrature technique for the k summation.

These basis functions were used to evaluate the hyperfine structure (hfs) of the Li^+ ion. The total hfs Hamiltonian $\mathcal{H}_{\rm hfs}$ is composed of three parts; namely, Fermi contact, dipole-dipole, and magnetic orbital terms. These three terms are given by

$$\mathcal{H}_c = \frac{16\pi}{3}\,\frac{\mu_B\mu_N}{Ia_B^3}\,\vec{I}\cdot\sum_i \vec{S}_i\delta(\vec{r}_i) , \tag{9a}$$

$$\mathcal{H}_d = 2\,\frac{\mu_B\mu_N}{Ia_B^3}\,\vec{I}\cdot\sum_i\left(\frac{3(\vec{s}_i\cdot\vec{r}_i)\vec{r}_i}{r_i^5}-\frac{\vec{s}_i}{r_i^3}\right), \tag{9b}$$

$$\mathcal{H}_o = 2\,\frac{\mu_B\mu_N}{Ia_B^3}\,\vec{I}\cdot\sum_i\frac{\vec{l}_i}{r_i^3} . \tag{9c}$$

In the experimental determination of atomic hfs, one uses the following spin Hamiltonian for these terms:

$$\mathcal{H}_\alpha^{\rm spin} = A_\alpha\vec{I}\cdot\vec{J} , \tag{10}$$

where α stands for c, d, or o. For the $2\,^3P_2(m_J = 2)$ state of Li^+ ($1s2p$) ion, A_α is given by

$$A_\alpha = (1/2I)\langle\mathcal{H}_\alpha\rangle . \tag{11}$$

The evaluation of A_α thus involves a calculation of the expectation value of $\mathcal{H}_\alpha$. This evaluation of expectation values is carried out according to Eq. (6).

Various terms in Eq. (6) can be represented by diagrams similar to Feynman diagrams. These diagrams are grouped according to the two integers m and n appearing in the summation in Eq. (6). Diagrams which belong to particular values of m and n are referred to as (m,n) diagrams. In the diagrams, we represent $2s_z\delta(r)$, $s_z(3z^2-r^2)/r^5$, and l_z/r^3 as wiggly lines followed by letters c, d, and o, respectively. To obtain the contributions to A_α in MHz from an individual diagram evaluated in units of a_B^{-3}, one has to apply a multiplying factor

$$K_c = \frac{8\pi}{3}\left(\frac{\mu_B}{2ha_B^3}\right)\left(\frac{\mu_N}{I}\right)\times 10^{-6}$$

for A_c and a factor

$$K_d = 2\left(\frac{\mu_B}{2ha_B^3}\right)\left(\frac{\mu_N}{I}\right)\times 10^{-6}$$

for A_d and A_o. The numerical values of K_c and K_d for $^6Li^+$ are 164.244 and 39.21, respectively. In the present calculation we have included all the diagrams up to the second order in electron-electron interaction. The more important diagrams are shown in Figs. 1–4. All the numbers appearing with these diagrams are given in MHz units and refer to ^6Li. To get the corresponding values for ^7Li, one has to multiply the values for ^6Li by the ratio

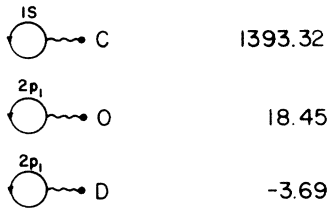

FIG. 1. Zero-order (0,0) diagrams for the hyperfine coupling constants (MHz).

$$(\mu_N/I)_{^7\mathrm{Li}}/(\mu_N/I)_{^6\mathrm{Li}} = 2.641 .$$

The zero-order diagrams are illustrated in Fig. 1. The orbital and dipole interactions together contribute only 14.75 MHz, which is about 1% of the contact contribution of 1393.32 MHz. Figure 2 depicts the (0,1) diagrams where these diagrams exist only for A_d. The net contribution is −0.04 MHz, which is about 1% of the zero-order dipole contribution of −3.69 MHz. In Fig. 3 we have the leading second-order contact diagrams. The four diagrams in the first row are (1,1) diagrams and the four in the second row are (0,2) diagrams. All these diagrams represent the mutual polarization effects of $1s$ and $2p$ electrons. The contribution to A_c from each diagram is indicated under the corresponding diagram. A similar set of diagrams are shown in Fig. 4. These are the leading second-order diagrams for the dipole and orbital operators. The first number under each diagram is the contribution to A_d and the second number is the contribution to A_o. We have summarized our final result for the nonrelativistic calculation in Table I. Final results of A_c, A_d, and A_o for $^6Li^+$ are 1391.02, −3.74, and 18.42 MHz, respectively.

Correlation effects are found to be very small. Thus, in the case of A_c, the total correlation contribution is −2.3 MHz, which is only 0.16% of the (0,0) contribution. Since we estimate the accuracy of our correlation results to be about 5%, the relativistic and radiative corrections are significant in making comparisons with experiment. In fact, the effect of these corrections turns out to be about the same order of magnitude as the correlation effects among electrons. The evaluation of these corrections followed the prescriptions and pertinent formulas in Rosner and Pipkin's paper[3] on ^{3}He and the results are summarized in Table II in terms of ppm with respect to the (0,0) contribution of A_c. We did not estimate such corrections for A_d and A_o, or for the higher-order contributions to A_c, since these quantities themselves are orders of magnitude smaller than the zero-order contribution to A_c. The reduced mass correction arises from the motion of the nucleus which has finite mass. This correction is smaller than in ^{3}He because of the larger mass of ^{6}Li and is even smaller for ^{7}Li. The relativistic correction is obtained[13] using a Dirac hydrogenic function for the $1s$ states with effective charge $\zeta = 3$. The radiative correction arises mainly from the anomalous magnetic moment of the electron, but other smaller radiative corrections have also been included using Eq. (13) of Ref. 3. Since the estimations of the contributions of these effects are based on a hydrogenic approximation for the $1s$ orbital, one should make some corrections for this. However, these corrections are not expected to be of an order greater than 10 ppm, the same order as the correction due to neutron and proton distributions which have not been included. In our theoretical treatment, where we use the actual hyperfine Hamiltonian, which is a sum over individual electrons, there is no adiabatic correction to be included. The final results for A_c, A_d, and A_o, including the above-mentioned corrections, are shown in Table III.

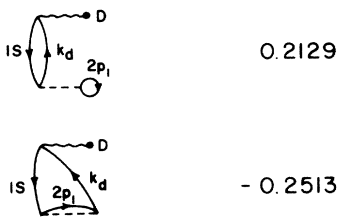

FIG. 2. First-order (0,1) diagrams for the dipolar coupling constant A_d (MHz).

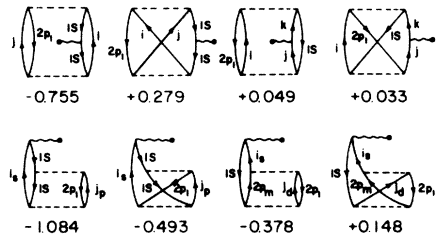

FIG. 3. Second-order (1,1) and (0,2) diagrams for the contact coupling constant A_c (MHz).

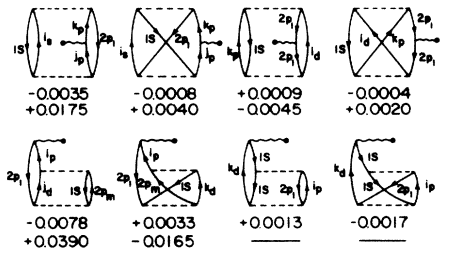

FIG. 4. Second-order contributions to the orbital A_o and dipolar A_d coupling constants (MHz). The first number refers to A_d and the second number to A_o.

TABLE I. Theoretical hyperfine coupling constants (Mhz).

Diagrams	A_c	A_d	A_o
(0, 0)	1393.32	−3.69	18.45
(0, 1)		−0.04	
Figs 3 and 4	−2.20	−0.01	0.04
Other diagrams	−0.10	0.00	−0.07
Total	1391.02	−3.74	18.42

III. HYPERFINE INTERACTION IN AN EXTERNAL MAGNETIC FIELD

In relating the predictions of the theory to Zeeman splittings in a magnetic field, we have to study the energy levels including fine-structure and hyperfine-structure effects in a magnetic field. In the presence of external magnetic fields, the spin-dependent Hamiltonian of an atomic system can be written

$$\mathcal{H}_s = \mathcal{H}_{\rm fs} + \mathcal{H}_{\rm hfs} + \mathcal{H}_Z . \tag{12}$$

The first term in Eq. (12) is the fine-structure (fs) Hamiltonian, which is given by

$$\mathcal{H}_{\rm fs} = \frac{\alpha^2}{2}\left[\left(\frac{Z\vec{l}_1}{r_1^3} - \frac{\vec{r}_{12}\times\vec{P}_1}{r_{12}^3} + \frac{2\vec{r}_{12}\times\vec{P}_2}{r_{12}^3}\right)\cdot\vec{s}_1 + \left(\frac{Z\vec{l}_2}{r_2^3} - \frac{\vec{r}_{21}\times\vec{P}_2}{r_{12}^3} + \frac{2\vec{r}_{21}\times\vec{P}_1}{r_{12}^3}\right)\cdot\vec{s}_2\right] + \alpha^2\left(\frac{\vec{s}_1\cdot\vec{s}_2}{r_{12}^3} - \frac{3(\vec{s}_1\cdot\vec{r}_{12})(\vec{s}_2\cdot\vec{r}_{12})}{r_{12}^5}\right). \tag{13}$$

The second term in Eq. (12) is the hfs Hamiltonian and is defined in Eq. (9). The last term represents the Zeeman interaction and is given by

$$\mathcal{H}_Z = g_s\mu_B\vec{S}\cdot\vec{B} + \mu_B\vec{L}\cdot\vec{B} - g_I\mu_N\vec{I}\cdot\vec{B} . \tag{14}$$

Various Zeeman sublevels can then be found by diagonalizing $\mathcal{H}_s$ in the basis of $|I\,^3P_J; FM_F\rangle$.

First we consider the fine-structure Hamiltonian $\mathcal{H}_{\rm fs}$. Its diagonal matrix elements are given by

$$W_J = \langle I\,^3P_J; FM_F|\mathcal{H}_{\rm fs}|I\,^3P_J; FM_F\rangle = AK + B[3K(2K+1) - 4L(L+1)], \tag{15}$$

where

$$A = \frac{\alpha^2}{4}\langle^3P|Z\left(\frac{l_{1z}}{r_1^3} + \frac{l_{2z}}{r_2^3}\right) - \frac{3}{r_{12}^3}(l_{12z} + l_{21z})|^3P\rangle ,$$

$$B = \frac{\alpha^2}{2L(L+1)}\langle^3P|\frac{3\cos^2\theta_{12} - 1}{2r_{12}^3}|^3P\rangle ,$$

$$K = \tfrac{1}{2}[J(J+1) - L(L+1) - S(S+1)] ,$$

$$l_{ijz} = [(\vec{r}_{ij}\times(\vec{P}_i - \vec{P}_j))]_Z .$$

TABLE II. Radiative and relativistic corrections to the hyperfine constant A_c in ppm with respect to the (0, 0) contribution to A_c.

Origin	^{6}Li	^{7}Li
Reduced mass	−273.7	−234.7
Rel. wave function	717.9	717.9
Q.E.D.	839.0	839.0
Rel. reduced mass	−6.2	−5.4
Total	1277.0 (1.78 MHz)	1316.8 (4.84 MHz)

The numerical values of W_J have been obtained from the theoretical calculation of Shiff *et al.*[14] With the following splittings

$$W_0 - W_1 = 5.19443\ \text{cm}^{-1} ,$$

$$W_1 - W_2 = -2.08988\ \text{cm}^{-1} ,$$

and the relation

$$W_0 + 3W_1 + 5W_2 = 0 ,$$

we find

$$W_0 = 3.45623\ \text{cm}^{-1} = 103.6152\ \text{GHz} ,$$
$$W_1 = -1.73820\ \text{cm}^{-1} = -52.1099\ \text{GHz} , \tag{16}$$
$$W_2 = 0.35168\ \text{cm}^{-1} = 10.5431\ \text{GHz} .$$

The matrix elements of the hfs Hamiltonian can be written in terms of the contact, dipolar, and orbital hyperfine constants A_c, A_d, and A_o, which have been evaluated theoretically in Sec. II:

$$\langle I\,^3P_J; FM_F|\mathcal{H}_{\rm hfs}|I\,^3P_J; FM_F\rangle = \{A_c + A_0 - \tfrac{1}{2}[16 - 3J(J+1)]A_d\}\vec{I}\cdot\vec{J}$$

$$\langle I\,^3P_{J+1}; FM_F|\mathcal{H}_{\rm hfs}|I\,^3P_J; FM_F\rangle = \frac{M_{J+1,J}}{2(J+1)}\{A_c - A_0 - \tfrac{1}{2}[3J(J+2) - 5]A_d\} , \tag{17}$$

where

$$M_{J+1,J} = \left(\frac{(F+J+I+2)(J+I+1-F)(F+J+1-I)(F+I-J)(J+4)(J+1)^2(2-J)}{(2J+1)(2J+3)}\right)^{1/2} ,$$

$$\vec{I}\cdot\vec{J} = \tfrac{1}{2}[F(F+1) - J(J+1) - I(I+1)] .$$

If one had ignored correlation effects in the evaluation of A_d and A_o, that is, assumed the same $\langle 1/r^3\rangle_{\rm av}$ factor for both of these quantities,[10] then these matrix elements would be equivalent to those given by

TABLE III. Net hyperfine coupling constants (MHz).

System \ Term	A_c	A_d	A_o
$^6Li^+$	1392.80	−3.74	18.42
$^7Li^+$	3678.40	−9.86	48.62

TABLE IV. Number of matrices for the hyperfine interaction in an external magnetic field.

M_F	$^6Li^+$ ($I=1$) Submatrices	M_F	$^7Li^+$ ($I=\frac{3}{2}$) Submatrices
0	one 7×7	$\pm\frac{1}{2}$	two 8×8
±1	two 6×6	$\pm\frac{3}{2}$	two 6×6
±2	two 3×3	$\pm\frac{5}{2}$	two 3×3
±3	two 1×1	$\pm\frac{7}{2}$	two 1×1

Lurio, Mandel, and Novick in the Russell-Saunders limit.[15] Note that $\mathcal{H}_{hfs}$ is diagonal with respect to F and M_F.

Finally, the matrix elements of $\mathcal{H}_Z$ are given by

$$\langle I^3P_J; FM_F|\mathcal{H}_Z|I^3P_J; FM_F\rangle = g_F\mu_B B_Z M_F\,,$$

$$\langle I^3P_J; F+1M_F|\mathcal{H}_Z|I^3P_J; FM_F\rangle = (g_I'+g_J)\frac{\mu_B B_z}{2(F+1)} \times\left(\frac{[(F+1)^2-M_F^2](F+J+I+2)(F+J+1-I)(F+I+1-J)(J+I-F)}{(2F+1)(2F+3)}\right)^{1/2},$$

$$\langle I^3P_{J+1}; FM_F|\mathcal{H}_Z|I^3P_J; FM_F\rangle = (g_s-1)\frac{\mu_B B_z M_F M_{J+1,J}}{4(J+1)F(F+1)}\,, \tag{18}$$

$$\langle I^3P_{J-1}; F+1M_F|\mathcal{H}_Z|I^3P_J; FM_F\rangle = (g_s-1)\frac{\mu_B B_z}{4J(F+1)} \times\left(\frac{[(F+1)^2-M_F^2](J+I-F-1)(J+I-F)(F+I+1-J)(F+I+2-J)(J+3)J^2(3-J)}{(2F+1)(2F+3)(2J-1)(2J+1)}\right)^{1/2},$$

$$\langle I^3P_{J+1}; F+1M_F|\mathcal{H}_Z|I^3P_J; FM_F\rangle = -(g_s-1)\frac{\mu_B B_z}{4(J+1)(F+1)} \times\left(\frac{[(F+1)^2-M_F^2](F+J+I+2)(F+J+I+3)(F+J+1-I)(F+J+2-I)(J+4)(J+1)^2(2-J)}{(2J+1)(2J+3)(2F+1)(2F+3)}\right)^{1/2}.$$

In these equations we have used the following symbols:

$$g_F = [F(F+1)]^{-1}[g_J\vec{\mathbf{F}}\cdot\vec{\mathbf{J}} - g_{I'}\vec{\mathbf{F}}\cdot\vec{\mathbf{I}}]\,,$$

$$g_J = \tfrac{1}{2}(g_S+1) \text{ for } L=S=1\,,$$

TABLE V. Energy levels in zero magnetic field (MHz).

Level	$^6Li^+$ Energy	Level	$^7Li^+$ Energy
$J=0$ $F=1$	103,678	$J=0$ $F=\frac{3}{2}$	104,428
$J=2$ $F=3$	13,358	$J=2$ $F=\frac{7}{2}$	21,695
$J=2$ $F=2$	9,231	$J=2$ $F=\frac{5}{2}$	9,925
$J=2$ $F=1$	6,374	$J=2$ $F=\frac{3}{2}$	319
$J=1$ $F=2$	−50,776	$J=2$ $F=\frac{1}{2}$	−5,885
$J=1$ $F=1$	−53,656	$J=1$ $F=\frac{5}{2}$	−47,686
$J=1$ $F=0$	−54,970	$J=1$ $F=\frac{3}{2}$	−57,627
		$J=1$ $F=\frac{1}{2}$	−61,850

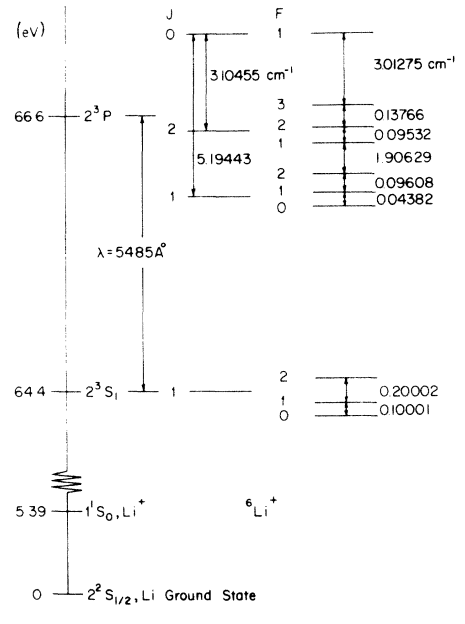

FIG. 5. Energy levels of $^6Li^+$ in zero magnetic field.

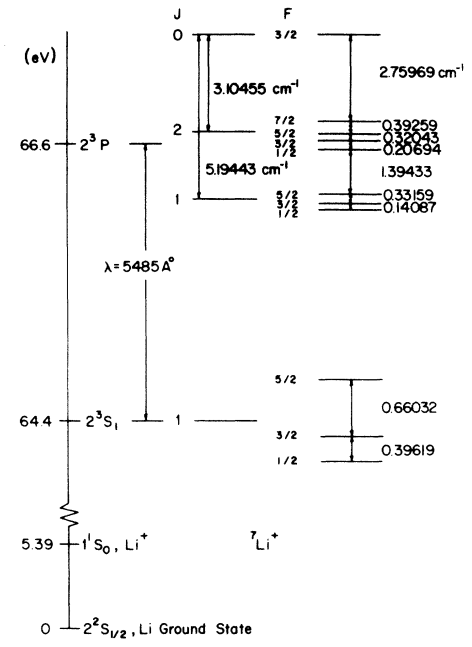

FIG. 6. Energy levels of $^7Li^+$ in zero magnetic field.

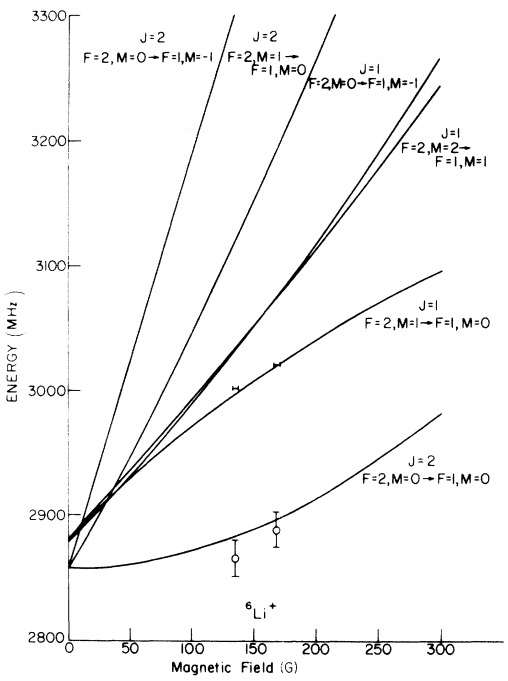

FIG. 7. Some transition frequencies for the $2\,^3P$ state of $^6Li^+$ in an external magnetic field. Experimental points indicated are for the $J=1$, $F=2$, $M=1\rightarrow J=1$, $F=1$, $M=0$ transition. The points labeled ⊢●⊣ are from Ref. 1, while the points labled ⊖ are extrapolated from the data of Ref. 2 (see text).

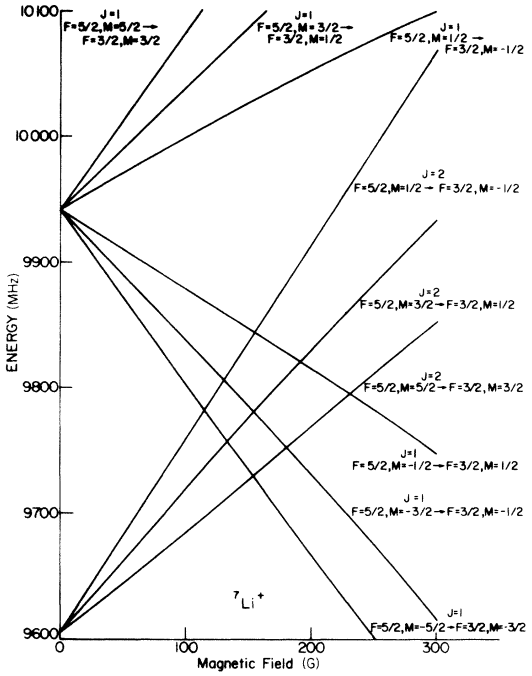

FIG. 8. Some transition frequencies for the $2\,^3P$ state of $^7Li^+$ in an external magnetic field.

$$g_{I'} = g_I(\mu_N/\mu_B),$$

$$g_s = 2.002\,319\,313,$$

the value of g_s being taken from a recent analysis.[16] These matrix elements are equivalent to those derived for the hydrogen molecule in the $c\,^3\Pi_u$ $(1s, 2p)$ state if one replaces $\vec{N}$ by $\vec{L}$ and the rotational factor g_N by 1 in the molecular expressions.[17–19] All other nondiagonal matrix elements can be obtained by using the Hermitean character of the operators involved. Furthermore, these matrix elements are seen to be diagonal in M_F. This enables one to reduce the total Hamiltonian matrix to direct sums of several smaller-size matrices for each case as shown in Table IV. These matrices are then diagonalized for each value of the magnetic field to give the energy levels.

In Table V, we list the energy levels in zero magnetic field. In Figs. 5 and 6, we summarize fine and hyperfine structures of $^6Li^+$ and $^7Li^+$. The electronic energy levels were taken from Herzberg and Moore.[20] In these figures, the results for the fine-structure splittings are from Schiff *et al.*,[14] and the hyperfine splitting for the $2\,^3S_1$ state was obtained from Breit-Doermann's formula[21] with the $(1+\epsilon)$ factor calculated by Luke *et al.*[22] For a nonzero magnetic field, we have plotted transition frequencies versus magnetic field. These are shown in Figs. 7 and 8 for

TABLE VI. Comparison of the theoretical hyperfine splittings with the calculated and observed splittings of Berry *et al.* (Ref. 2) (MHz).

	Hyperfine transition		This paper	Ref. 2	
	JF	$J'F'$		Obs.	Calc.
$^6Li^+$	22	21	2858		2769
	12	11	2880		2750
	23	22	4127		3999
	12	10	4194		3999
$^7Li^+$	$1\frac{3}{2}$	$1\frac{1}{2}$	4223		3965
	$2\frac{3}{2}$	$2\frac{1}{2}$	6204	6010	5984
	$2\frac{5}{2}$	$2\frac{3}{2}$	9606		9255
	$1\frac{5}{2}$	$1\frac{3}{2}$	9941		9462
	$2\frac{7}{2}$	$2\frac{5}{2}$	11 770	11 320	11 347
	$1\frac{5}{2}$	$1\frac{1}{2}$	14 164	13 700	13 427
	$2\frac{5}{2}$	$2\frac{1}{2}$	15 810	15 000	15 233

$^6Li^+$ and $^7Li^+$, respectively. In the case of $^6Li^+$, we have also shown the experimental results.[1,2]

IV. DISCUSSION

The agreement between theory and the experimental results of Adler *et al.*[1] is very good as seen in Fig. 7. However, the agreement with the energy levels obtained from the beam-foil experiments by Berry *et al.*[2] for the $2\,^3P$ states of $^6Li^+$ and $^7Li^+$ is not good as evidenced in Table VI. The disagreement varies from 6% to 3%. Some of the variance between our theoretical hyperfine splittings and the calculated values of Berry *et al.* can be attributed to their fitting the experimental data to just the contact part of the spin Hamiltonian [Eq. (10)] which completely ignores the influence of the $2p$ electron. Since the contact interaction is so large, this approximation cannot account for more than 2%. What is more disconcerting is the differences between our theoretical hyperfine splittings and their observed splittings for $^7Li^+$, which vary from 5% to 3%, whereas they claim that their frequencies are accurate to 1%. They do not report similarly observed splittings for $^6Li^+$ with which we can compare. The theoretical splittings are expected to be of a high precision, since we have included all the important corrections due to many-body, radiative, relativistic, mass-motion and other important corrections. Since these corrections are themselves much smaller than the difference between the predictions of our theory and the beam-foil experiments, this disagreement is quite serious. Berry is now engaged in a more accurate experimental determination of the hyperfine splittings in the $2\,^3P$ state of Li^+.[23]

As regards to a comparison between the two sets of experimental results themselves, this cannot be done directly, since Adler *et al.* did their measurements at 136 and 168 G. However, with the methods outlined in Sec. III, we can take the zero-field splittings of Berry *et al.* and extrapolate them to these magnetic fields. In Fig. 7 we have also plotted these points and it is seen that the results of the two experiments differ by 4%. In contrast, our theory and the experimental results of Adler *et al.* are in excellent agreement.

From Table I we see that the correlation effects are very small and the coupling constants are predominantly determined by the one-electron terms, which is not surprising for this two-electron system where the tightly bound unpaired $1s$ electron makes the major contribution to hyperfine structure. The relativistic corrections (Table II) are of the same magnitude as the correlation terms. This work represents a very precise calculation of the hyperfine splittings as a function of an external magnetic field, and it is hoped that it will be some utility in resolving the differences between the two experimental measurements.

†Partially supported by the National Science Foundation and the Naval Ordance Systems Command, U. S. Department of the Navy under Contract No. N00017-72-C-4401.

[1]A. Adler, T. Lucatorto, R. Novick, and G. Sprott (unpublished). A brief description of the electron-impact-excitation technique for hyperfine structure and results on Zeeman splitting of Li^+ (^3P) state is available from the Columbia University, Department of Physics, Progress Report No. 19, August 1969 (unpublished).

[2]H. G. Berry, J. L. Subtil, E. H. Pinnington, H. J. Andrä, W. Wittman, and A. Gaupp, Phys. Rev. A 7, 1609 (1973).

[3]S. D. Rosner and F. M. Pipkin, Phys. Rev. A 1, 571 (1970).

[4]R. E. Watson and A. J. Freeman, *Hyperfine Interactions*, edited by A. J. Freeman and R. B. Frankel (Academic, New York, 1967).

[5]P. S. Bagus and J. Bauche, Phys. Rev. A 8, 734 (1973).

[6]E. S. Chang, R. T. Pu, and T. P. Das, Phys. Rev. 174, 1 (1968).

[7]H. P. Kelly, Phys. Rev. 180, 55 (1969).

[8]N. C. Dutta, C. Matsubara, R. T. Pu, and T. P. Das, Phys. Rev. Lett. 21, 1139 (1968).

[9]N. C. Dutta, C. Matsubara, R. T. Pu, and T. P. Das, Phys. Rev. 177, 33 (1969).

[10]J. D. Lyons, R. T. Pu, and T. P. Das, Phys. Rev. 178, 103 (1969).
[11]T. Lee, N. C. Dutta, and T. P. Das, Phys. Rev. A 1, 995 (1970).
[12]S. N. Ray, T. Lee, and T. P. Das, Phys. Rev. A 7, 1469 (1973).
[13]L. Tterlikkis, S. D. Mahanti, and T. P. Das, Phys. Rev. 176, 10 (1968).
[14]B. Schiff, Y. Accad, and C. L. Pekeris, Phys. Rev. A 1, 1837 (1970).
[15]A. Lurio, M. Mandel, and R. Novick, Phys. Rev. 126, 1758 (1962).
[16]Sara Granger and G. W. Ford, Phys. Rev. Lett. 28, 1479 (1972).
[17]A. N. Jette and P. Cahill, Phys. Rev. 160, 35 (1967).
[18]A. N. Jette, Phys. Rev. A 5, 2009 (1972).
[19]W. Lichten, Phys. Rev. A 3, 594 (1971).
[20]G. Herzberg and H. R. Moore, Can. J. Phys. 37, 1293 (1963).
[21]G. Breit and F. W. Doermann, Phys. Rev. 36, 1732 (1930).
[22]P. J. Luke, R. E. Meyerott and W. W. Clendenin, Phys. Rev. 85, 401 (1952).
[23]H. G. Berry (private communication).